THE ASTROPHYSICAL JOURNAL, 505:236–243, 1998 September 20

MODEL FOR ASTROPHYSICAL X-RAY ABSORPTION FINE STRUCTURE

ROBERT C. FORREY AND JONATHAN W. WOO
Harvard-Smithsonian Center for Astrophysics, Cambridge, MA 02138
AND
KYEONGJAE CHO
Mechanics and Computation Division, Mechanical Engineering Department, Stanford University, Stanford, CA 94305-4040
Received 1997 March 31; accepted 1998 April 23

ABSTRACT

We present a theoretical model and database designed to provide analysis of astrophysical X-ray absorption fine structure (XAFS). The model includes spherical wave corrections and multiple-scattering contributions to the modification of the X-ray absorption coefficient. The model and database provide the basis for the astrophysical XAFS analysis (AXA) tool, which may be used to analyze properties of interstellar grains and molecules from high-resolution X-ray spectra expected to be observed by future satellite missions (e.g., the Advanced X-ray Astrophysics Facility).

Subject headings: dust, extinction — galaxies: ISM — techniques: spectroscopic — X-rays: galaxies

1. INTRODUCTION

High-resolution ($E/\Delta E \sim 1000$) X-ray spectrometers on board future satellite missions (e.g., the Advanced X-ray Astrophysics Facility [AXAF]) have opened up a new window to study the properties of interstellar grains and molecules (Woo 1995). Analysis of the X-ray absorption fine structure (XAFS) in the observed spectra allows for a deeper probing of the interstellar medium than other traditional methods of study such as optical or near-optical astronomy (Martin 1970; Evans 1986). Since XAFS is produced by the interference of an outgoing photoelectron wave from a central atom with scattered waves from nearby atoms, it has the capability to provide detailed information about the type, structure, and state of the matter in the interstellar medium. In order to facilitate the use of XAFS to explore previously unknown properties of interstellar molecules and grains, we have initiated a project (Woo, Forrey, & Cho 1997) aimed at providing the astrophysics community with suitable theoretical tools and an easily accessible database for analyzing astrophysical spectra.

Much work has been done on XAFS by the condensed matter community in recent years (Muller & Schaich 1983; Gurman, Binsted, & Ross 1984; Barton & Shirley 1985; Rehr et al. 1986; McKale et al. 1988; Rehr & Albers 1990; Mustre de Leon et al. 1991; Rehr, Albers, & Zabinsky 1992; Zabinsky et al. 1995), and elaborate codes have been developed for the analysis of laboratory XAFS data (Filipponi et al. 1991; Newville et al. 1995). Spherical wave multiple-scattering (SWMS) theories have provided a framework that now appears capable of providing a complete account of the energy dependence of XAFS for laboratory samples. As a result, different strategies for including SWMS into the analysis of XAFS data have been implemented. Semi-empirical models have been developed that rely on experimental fitting parameters to compensate for theoretical errors. Sophisticated ab initio models designed to provide high-accuracy theoretical standards have also been developed (Rehr & Albers 1990; Mustre de Leon et al. 1991; Rehr et al. 1992). Our objective is to produce a simple model that includes the important physics needed for adequately describing astrophysical spectra. In constructing a model for astrophysical XAFS, we anticipate structural differences to exist between interstellar molecules and grains and laboratory samples. We expect thermal disorder, which normally smears out much of the fine detail of photoabsorption spectra at room temperature, to play a less significant role at the low temperatures of the interstellar medium. An efficient determination of SWMS is necessary for allowing extraction of detailed information on the static structural disorder of astrophysical grains and molecules. Therefore, we use a hybrid approach that retains much of the simplicity of semiempirical models while at the same time incorporates many of the advances of full ab initio SWMS theories. The model has sufficient flexibility to simulate an arbitrary chemical environment. It supports different levels of approximation and permits the ready determination of energies and geometries at which the effects of multiple scattering become significant.

We solve the relativistic Kohn-Sham equation self-consistently to get the electron density function for any atomic system of interest. A complex self-energy potential (Hedin & Lundqvist 1969) is constructed from the density function, and the Schrödinger equation containing the self-energy potential is solved numerically for the individual scattering amplitudes. Electron scattering in a molecule or solid is described using a multiple-scattering formulation with a standard "muffin-tin" procedure to account for the surrounding atoms. At low energies the scattering amplitudes include spherical wave effects that depend on the interatomic distance. The single-scattering contributions are described by the exact spherical wave formulation of Rehr et al. (1986). Multiple scattering is incorporated into the model using an approximate spherical wave treatment. The high-energy extended XAFS (EXAFS) can be described by using exact spherical waves or by the usual plane wave approximation (PWA) with an energy shift.

In our previous work (Woo et al. 1997), we presented the astrophysical EXAFS analysis (AEA) tool. Here we present the more general astrophysical XAFS analysis (AXA) tool. As before, we have designed the tool so that a user with a limited understanding of the theoretical aspects of numerical modeling can easily access the database and use it to study XAFS within a limited personal/workstation computer facility. We note that the tools may also be useful for

calibrating X-ray spectrometers that must account for XAFS in their instrumental response (e.g., Owens et al. 1997). The details of the theoretical model are presented in § 2. In § 3 we describe the AXA tool and provide some numerical examples.

2. THEORETICAL XAFS MODEL

The theoretical formulation of XAFS can be found in many articles (see, e.g., Lee & Pendry 1975), so we give only a brief outline of the theory here. Since it is our hope that the present model will provide a foundation for analyzing astrophysical XAFS, we have included complete derivations that make clear all approximations that are made.

The oscillatory absorption coefficient normalized to a smooth absorption coefficient μ_0 of an isolated atom is given by

$$\chi = \frac{\mu - \mu_0}{\mu_0}, \tag{1}$$

where μ is the absorption coefficient of the center atom of the many-atom system (molecule or condensed matter). The X-ray absorption coefficient μ can be calculated by Fermi's Golden Rule within the dipole approximation for the photon-induced transition of an electron from initial state $|i\rangle$ to a final state $|f\rangle$:

$$\mu \sim |\langle f|\hat{\epsilon}\cdot\boldsymbol{r}|i\rangle|^2, \tag{2}$$

where $\hat{\epsilon}$ is the polarization vector of the photon and $\boldsymbol{r}$ is the electron coordinate. For an isolated atom, the final state consists of an ionized atom plus an ejected photoelectron. For a multiatomic system, the final state is defined by

$$|f\rangle = \sum_{lm} (1 + M_{lm})|lm\rangle, \tag{3}$$

where M_{lm} gives the modification of the final state due to scattering from the neighboring atoms. Using equations (2) and (3) gives the general expression

$$\mu \sim \sum_{lm}\sum_{l'm'} \langle i|\hat{\epsilon}\cdot\boldsymbol{r}|lm\rangle\langle l'm'|\hat{\epsilon}\cdot\boldsymbol{r}|i\rangle(1 + M_{lm})(1 + M^*_{l'm'}). \tag{4}$$

The random orientation of atoms in the sample is taken into account by averaging over the X-ray beam direction using

$$\hat{\epsilon}\cdot\hat{r} = \tfrac{1}{3}\sum_m Y^*_{1m}(\hat{\epsilon})Y_{1m}(\hat{r}), \tag{5}$$

which yields

$$\mu \sim \sum_{lm} |\langle i|rY_{10}|l\rangle|^2(1 + M_{lm} + M^*_{lm} + |M_{lm}|^2). \tag{6}$$

The scattered waves are generally weak enough that the squared term in equation (6) can be neglected. The final angular momentum is determined by the selection rule $l = l_i \pm 1$. For cases where both final angular momentum states are allowed, the $l = l_i + 1$ term always dominates the $l = l_i - 1$ term (Gurman et al. 1984). Therefore, the sum over angular momentum in equation (6) can generally be replaced by one term. The definition in equation (1) is then used to get the oscillatory absorption coefficient

$$\chi_l(k) = 2\,\mathrm{Re}\left(\sum_m M_{lm}\right). \tag{7}$$

For a K-edge transition, $|i\rangle$ is the 1s core state of the X-ray–absorbing atom and $l = 1$. In general, the matrix element M_{lm} can be expressed as (Lee & Pendry 1975)

$$M_{lm} = \frac{1}{2l+1} Z_{lm,lm} e^{2i\delta_l}, \tag{8}$$

where δ_l is the central atom phase shift, and $Z_{lm,l'm'}$ is the transition matrix connecting the outgoing wave at the central atom with the interfering wave produced by scattering from neighboring atoms. The unknown $Z_{lm,l'm'}$ can be evaluated by expanding in a multiple-scattering series

$$Z_{lm,l'm'} = \sum_{\text{paths}} [Z^{(1)}_{lm,l'm'} + Z^{(2)}_{lm,l'm'} + \cdots], \tag{9}$$

where the summation is over all possible paths and the superscript indicates the number of collisions. Using the PWA to get the single-scattering term $Z^{(1)}_{1m,1m}$ gives the usual EXAFS formula

$$\chi_1(k) = -\mathrm{Im}\sum_{\text{paths}} f(\pi)\frac{\exp(2ikr + 2i\delta_1)}{kr^2} e^{-2\sigma^2k^2}, \tag{10}$$

where

$$f(\theta) = \frac{1}{2ik}\sum_{l=0}^{\infty}(2l+1)(S_l - 1)P_l(\cos\theta) \tag{11}$$

is the scattering amplitude and σ is a Debye-Waller factor. For astrophysical grains, thermal vibrations due to the cold temperatures of interstellar space (e.g., $T \sim 10$–100 K) should be negligible. Therefore, we expect that Debye-Waller factors for astrophysical XAFS will contain detailed information on the static structural disorder of the grains, particularly in the low-energy part of the spectrum. To accurately describe the low-energy spectra, it is necessary to include spherical wave corrections and multiple-scattering effects into the XAFS model.

2.1. *Spherical Waves*

Spherical wave corrections to the PWA for XAFS have been successful in explaining discrepancies between theory and experiment for low energies (Muller & Schaich 1983; Rehr et al. 1986; Rehr & Albers 1990). In the present work, we use the spherical wave approximation (SWA) of Rehr et al. (1986). The single-scattering term of equation (9) is obtained from the expansion

$$Z^{(1)}_{lm,l'm'} = \tfrac{1}{4}\sum_{l''m''} G_{lm,l''m''}(-\boldsymbol{r})(S_{l''} - 1)G_{l''m'',l'm'}(\boldsymbol{r}), \tag{12}$$

where $\boldsymbol{r}$ is the position of the neighboring atom from the center atom, S_l is the scattering matrix element, and $G_{lm,l'm'}(\boldsymbol{r})$ is the free propagator

$$G_{lm,l'm'}(\boldsymbol{r}) = 4\pi Y^*_{l0}(\hat{r})Y_{l'0}(\hat{r})\frac{e^{ikr}}{kr} g^{(|m|)}_{ll'}(kr)\delta_{mm'}, \tag{13}$$

where $\boldsymbol{r}$ has been chosen to lie along the z-axis and $g^{(|m|)}_{ll'}(kr)$ is a radial function derived in Appendix A. For an s-wave initial state, $l = 1$ and the result is

$$\sum_m Z^{(1)}_{1m,1m} = -3f(r,\pi)\frac{\exp(2ikr)}{2ikr^2}, \tag{14}$$

where

$$f(r, \theta) = \frac{1}{2ik} \sum_{l=0}^{\infty} (2l+1)(S_l - 1)P_l(\cos\theta) \times \left[\frac{(l+1)c_{l+1}^2(kr) + lc_{l-1}^2(kr)}{2l+1}\right]. \quad (15)$$

The function $c_l(x) = i^l x \exp(-ix)h_l^{(+)}(x)$ is defined by $h_l^{(+)}(x) = ih_l^{(1)}(x)$ where $h_l^{(1)}(x)$ is a spherical Hankel function of the first kind. We note that since the free Green's function, equation (13), is exact, the SWA given by equation (14) is an exact first-order spherical wave-scattering theory. Approximate spherical wave theories such as the point-scattering approximation (PSA) can be derived by assuming that the Green's function has the separable form

$$\tilde{G}_{lm,l'm'}(\boldsymbol{r}) = 4\pi Y_{lm}^*(\hat{r})Y_{l'm'}(\hat{r}) \frac{e^{ikr}}{kr} c_l(kr)c_{l'}(kr) . \quad (16)$$

Using equations (12) and (16), it is easy to show that the PSA is equivalent to replacing the SWA formulae, equations (14) and (15), with

$$\sum_m \tilde{Z}_{1m,1m}^{(1)} = -3\tilde{f}(r, r, \pi)c_1^2(kr) \frac{\exp(2ikr)}{2ikr^2} \quad (17)$$

and

$$\tilde{f}(r, r', \theta) = \frac{1}{2ik} \sum_{l=0}^{\infty} (2l+1)(S_l - 1)P_l(\cos\theta)c_l(kr)c_l(kr') . \quad (18)$$

For comparison, the PSA of Lee & Pendry (1975) is given by the effective spherical wave amplitude (see Appendix B)

$$\tilde{f}(r, \theta) = \frac{1}{2ik} \sum_{l=0}^{\infty} (2l+1)(S_l - 1)P_l(\cos\theta)c_l(kr) . \quad (19)$$

In the high-energy limit, the asymptotic expansion $h_l^{(1)}(kr) \sim (-i)^{l+1} \exp(ikr)/kr$ implies that $c_l(kr) \sim 1$, and the SWA and PSA amplitudes equations (15), (18), and (19) reduce to the usual PWA amplitude $f(\theta)$ given in equation (11).

2.2. *Multiple Scattering*

The multiple-scattering terms of expansion equation (9) are defined by assuming that the photoelectron is scattered first by an atom located at $\boldsymbol{r}_1$, followed by an atom located at $\boldsymbol{r}_2$, and so on. The exact double-scattering term $Z_{lm,l'm'}^{(2)}$ is obtained from the following generalization of equation (12):

$$Z_{lm,l'm'}^{(2)} = \frac{1}{8i} \sum_{l_1m_1} \sum_{l_2m_2} G_{lm,l_2m_2}(-\boldsymbol{r}_2)(S_{l_2} - 1) \times G_{l_2m_2,l_1m_1}(\boldsymbol{r}_2 - \boldsymbol{r}_1)(S_{l_1} - 1)G_{l_1m_1,l'm'}(\boldsymbol{r}_1) \quad (20)$$

Higher order multiple-scattering terms are similarly obtained. For diatomic molecules, the even-order multiple-scattering terms are absent, and the odd-order terms can be obtained recursively from

$$Z_{lm,l'm'}^{(n)} = -\sum_{l''m''} Z_{lm,l''m''}^{(n-2)}(S_{l''} - 1)Z_{l''m'',l'm'}^{(1)} , \quad (21)$$

where $Z_{lm,l'm'}^{(1)}$ is evaluated from equation (A5). We note that equation (21) provides an exact spherical wave treatment of multiple scattering for diatomic molecules. For large molecules and crystals, the multiple-scattering contributions to XAFS such as equation (20) are difficult to analyze and compute because of angular momentum coupling. Therefore, we use the separable PSA propagator equation (16) when considering double and higher order multiple-scattering contributions for such systems. The second-order result is

$$\sum_m \tilde{Z}_{lm,lm}^{(2)} = -(2l+1)P_l(\cos\theta)\tilde{f}(r_1, r_{12}, \theta_1) \times \tilde{f}(r_2, r_{12}, \theta_2)c_l(kr_1)c_l(kr_2) \times \frac{\exp[ik(r_1 + r_2 + r_{12})]}{2ikr_1r_2r_{12}} , \quad (22)$$

where θ_1 is the angle between $\boldsymbol{r}_1$ and $\boldsymbol{r}_{12}$, which arises from the first collision, θ_2 is the angle between $\boldsymbol{r}_{12}$ and $\boldsymbol{r}_2$, which arises from the second collision, and $\theta = \theta_1 + \theta_2 - \pi$. Extension to higher order scattering is straightforward. The usual PWA (see Appendix B) is recovered in the high-energy limit

$$\sum_m Z_{lm,lm}^{(2)} = -(2l+1)P_l(\cos\theta)f(\theta_1)f(\theta_2) \times \frac{\exp[ik(r_1 + r_2 + r_{12})]}{2ikr_1r_2r_{12}} . \quad (23)$$

For the K-edge

$$\chi_1(k) = -\mathrm{Im} \sum_{\text{paths}} e^{2i\delta_1}\left[f(\pi)\frac{\exp(2ikr_1)}{kr_1^2} + \cos\theta\, f(\theta_1) \times f(\theta_2)\frac{\exp[ik(r_1 + r_2 + r_{12})]}{kr_1r_2r_{12}} + \cdots\right]. \quad (24)$$

Normally, the individual terms of the expansion (24) can be analyzed separately using Fourier transform techniques. Therefore, it is conventional to define a length parameter L whose value determines what terms in equation (24) need to be considered. In the next section, we give an example that relates L to the number of terms in the multiple-scattering expansion (24).

3. AXA TOOL AND DATABASE

We have built the AXA tool to have the flexibility needed to calculate XAFS for any desired compound. The basic steps used by the AXA tool are as follows: The relativistic Kohn-Sham equation is solved self-consistently to get the density function for any atomic system of interest. Electron-atom scattering is described by replacing the Dyson equation for the single-particle Green's function by a Schrödinger equation with a complex self-energy potential. This step requires the use of the plasmon pole approximation in which the excitations of an electron gas are replaced by a single pole (Hedin & Lundqvist 1969). It has been shown (Lee & Beni 1977; Mustre de Leon et al. 1991) that the self-energy acts as an effective potential that adequately accounts for the exchange and correlation effects caused by the electrons in a single atom. The electron-atom scattering amplitudes are used within a multiple-scattering formulation that accounts for the surrounding atoms. The multiple-scattering method uses a standard muffin-tin procedure to isolate the individual atoms in the molecule or crystal. The Schrödinger equation containing the self-energy potential is solved numerically for the individual scattering amplitudes. The models include spherical wave effects that depend on the interatomic distance.

The database contains electron densities for all elements with atomic numbers up to 92. The AXA tool uses the electron density to compute the self-energy potential as a function of k in atomic units. The absorption coefficient $\chi(k)$ is then calculated in two steps. In the first step, the single-scattering contributions are computed from the interatomic distances and bond angles. The scattering amplitude is stored as a function of the shifted momentum $k \rightarrow [k^2 - V_{\mathrm{MT}}(k)]^{1/2}$, where $V_{\mathrm{MT}}(k)$ is the energy-dependent potential at the muffin-tin radius. In the second step, the central atom phase shift is computed and the desired multiple-scattering contributions are added. The present version of the AXA tool contains an input flag that determines which single-scattering approximation is to be used. Other inputs include the muffin-tin radius and energy threshold, which allow the user some flexibility when modeling XAFS.

3.1. *Spherical Wave Code*

In order to calibrate our spherical wave code, we studied the scattering amplitudes given by equations (11), (15), and (18) for Cu as a function of k. The muffin-tin radius was chosen to be half the interatomic distance of 4.8 a.u. The results, shown in Figure 1, are consistent with the calculations of Rehr et al. (1986). As expected, the scattering amplitude of equation (18) gives a better approximation to the exact spherical wave amplitude of equation (15) than does the usual PWA amplitude of equation (11). This is because equation (18) retains some spherical wave information because of the polynomial part of the outgoing spherical Hankel function, whereas equation (11) does not. The PSA agrees very well with the SWA above 4 a.u., whereas the PWA must shift the energy reference in order to obtain agreement. All of the amplitudes have a cusp at $k = 1$ a.u. because of the onset of plasmon excitations.

3.2. *Multiple-Scattering Code*

In order to test our multiple-scattering code, we studied the case of the O_2 molecule. Rehr et al. (1992) provided an interpretation of the σ^* shape resonance for O_2 based on high-order SWMS calculations. They found that the resonance was due to the constructive interference of many collisions between the two scattering centers. Using the PSA described above, we obtain results that are very similar to the exact SWMS calculations (Rehr et al. 1992). Figure 2 shows the weighted absorption coefficient $k^2\chi(k)$ as a function of k. The individual terms of the multiple-scattering expansion are shown in Figure 2*a*. The number n refers to the superscript in equation (9). At small values of k, the terms add together to enhance and sharpen the resonance. This is shown in Figure 2*b* where the partial sums are given through fifth order. For our calculations, the muffin-tin radius was chosen to be half the interatomic spacing of 2.28 a.u. and the energy threshold was assumed to be zero. The position of the resonance can be moved into agreement with experiment by shifting the energy threshold.

3.3. *Reduction of Variables*

One difficulty that typically arises in modeling XAFS data is dealing with many unknown variables. In order to reduce the number of variables in a multiple-scattering expansion, we have implemented some well-tested modeling ideas (Teo 1985). For example, we considered the case of a triatomic molecule in which atoms 1 and 2 are nearly colinear with the central atom 0 and $r_2 > r_1$. In this case, there are three separate paths that correspond to approx-

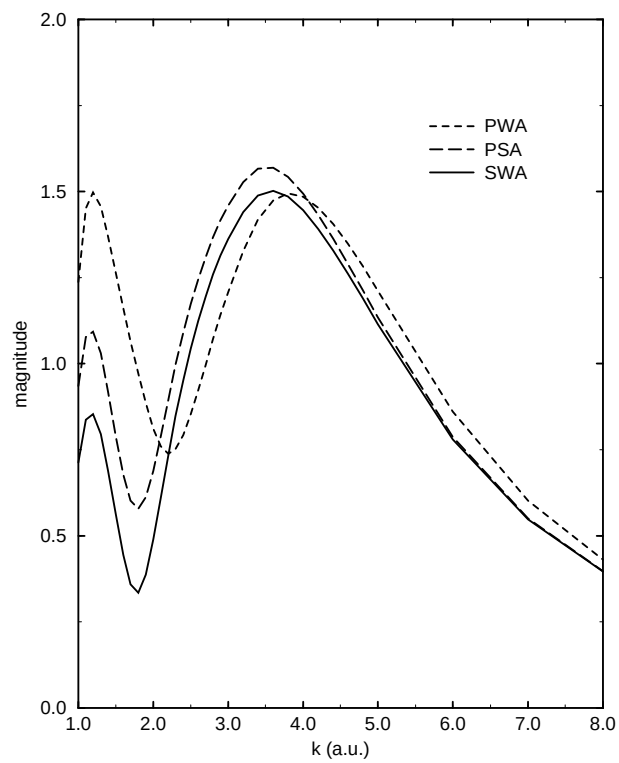

FIG. 1*a*

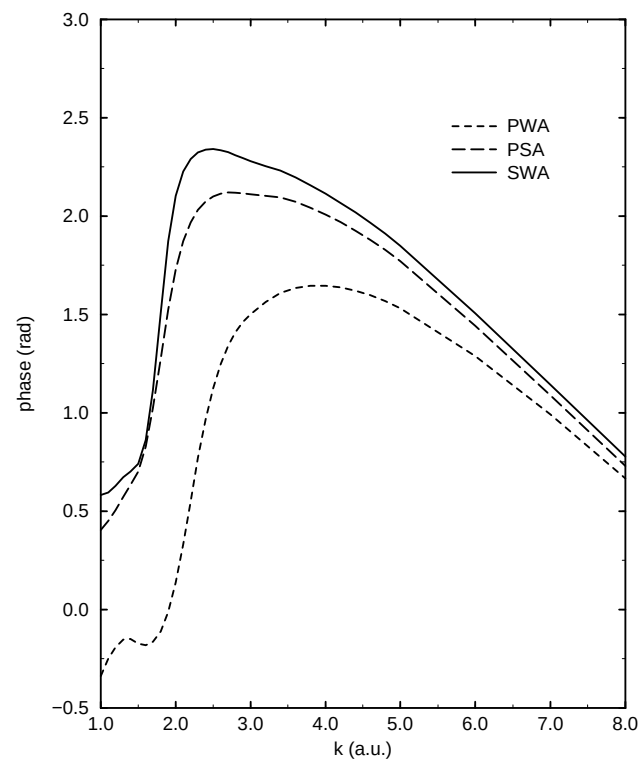

FIG. 1*b*

FIG. 1.—(*a*) Magnitude and (*b*) phase of the scattering amplitude approximations for copper. The dotted curve is $f(\pi)$ (eq. [11]), the dashed curve is $\tilde{f}(r,r,\pi)$ (eq. [18]), and the solid curve is $f(r, \pi)$ (eq. [15]).

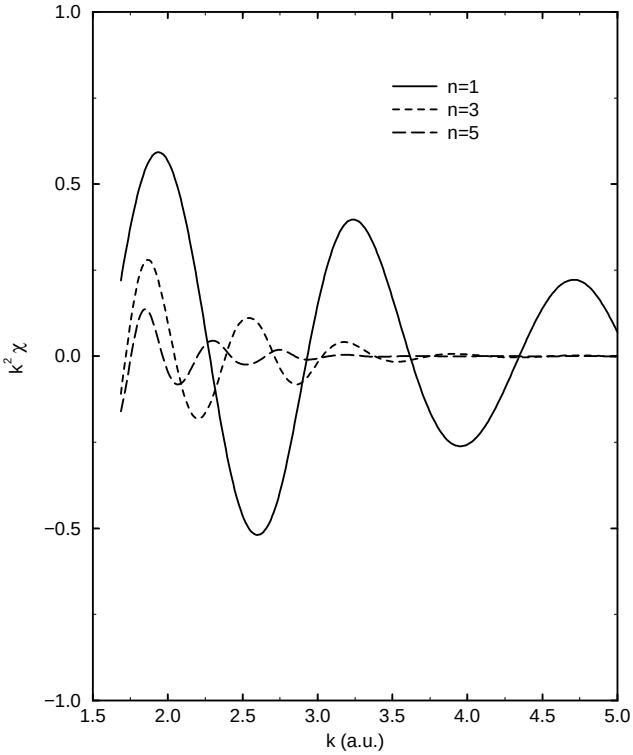

FIG. 2*a*

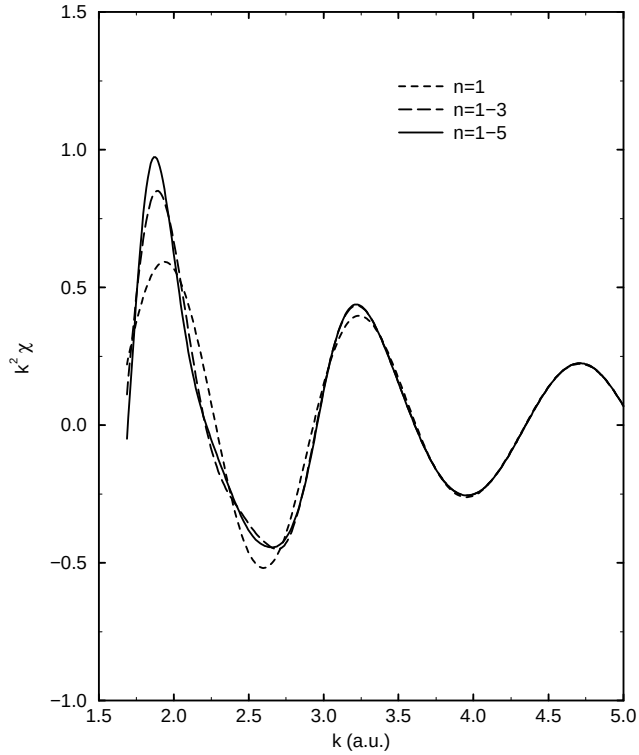

FIG. 2*b*

FIG. 2.—Weighted absorption coefficient $k^2\chi(k)$ for the O_2 molecule. The individual terms of the multiple-scattering expansion are shown in panel *a* and the partial sums are shown in panel *b*.

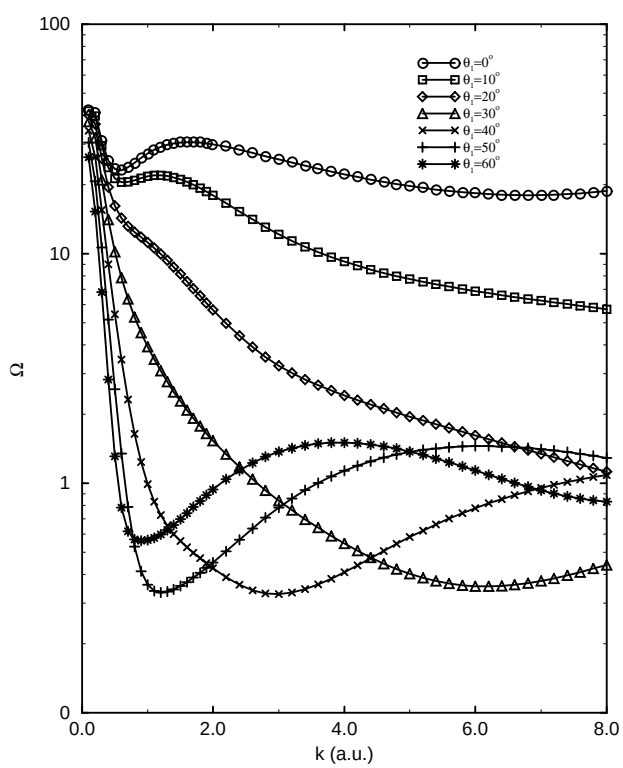

FIG. 3*a*

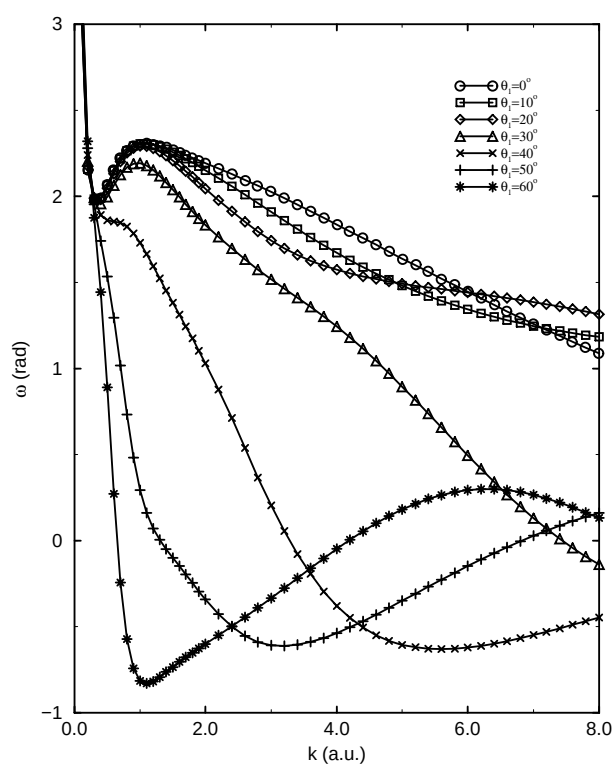

FIG. 3*b*

FIG. 3.—(*a*) Amplitude modification Ω and (*b*) phase modification ω due to multiple scattering in oxygen. The curves correspond to $\theta_1 = 0°$, $10°$, $20°, \ldots, 60°$.

imately the same path length L, namely, $L \approx 2r_2 \approx r_1 + r_2 + r_{12} \approx 2(r_1 + r_{12})$. The oscillatory absorption coefficient is therefore given by

$$\chi_1(k) = -\mathrm{Im}\, e^{2i\delta_1}\left\{ f(\pi)\,\frac{\exp\,(2ikr_2)}{kr_2^2} + 2\cos\theta\, f(\theta_1) \times f(\theta_2)\,\frac{\exp\,[ik(r_1 + r_2 + r_{12})]}{kr_1 r_2 r_{12}} + f(\theta_1) f(\pi) f(\theta_1)\,\frac{\exp\,[2ik(r_1 + r_{12})]}{kr_1^2 r_{12}^2}\right\}, \quad (25)$$

where the second term is counted twice since $0 \to 1 \to 2 \to 0$ gives the same contribution as $0 \to 2 \to 1 \to 0$. Following Teo (1985), we assume $\theta_1 \approx 0$ and $\theta_2 \approx \pi$, so that equation (25) can be rewritten as

$$\chi_1(k) = -\mathrm{Im}\, f(\pi)\,\frac{\exp\,(2ikr_2 + 2i\delta_1)}{kr_2^2} \times \left\{1 + \frac{r_2}{r_1 r_{12}}\, f(\theta_1)\exp\,[ik(r_1 - r_2 + r_{12})]\right\}^2 . \quad (26)$$

The definitions

$$\Omega = \left|1 + \frac{r_2}{r_1 r_{12}} f(\theta_1)\exp\,[ik(r_1 - r_2 + r_{12})]\right|^2 , \quad (27)$$

$$\omega = \arg\left\{1 + \frac{r_2}{r_1 r_{12}} f(\theta_1)\exp\,[ik(r_1 - r_2 + r_{12})]\right\}^2 \quad (28)$$

allow the multiple-scattering result to be expressed as a single-scattering term with a modified amplitude and phase. It was pointed out by Teo (1985) that although the above formulation was derived under the assumption $\theta_1 \approx 0$, it can also be used for large angles without introducing significant error into the calculation. Figure 3 shows Ω and ω as functions of θ_1 and k for the case of three oxygen atoms with $r_1 = 1.95$ Å and $r_{12} = 1.28$ Å. In these calculations, the muffin-tin potentials were overlapped (i.e., no muffin-tin radius was used), which contributes an error of a few eV (Lee & Beni 1977). Our results are consistent with earlier calculations by Teo (1985) when $\theta_1 > 10$. At smaller angles, however, we find stronger amplitude enhancement ($\Omega > 1$), probably due to differences in the self-energy potentials. At large angles, amplitude reduction ($\Omega < 1$) also occurs as a result of multiple scattering. The phase modification ω depends more weakly on θ_1 and k.

4. DISCUSSION

We have computed the single-scattering contribution to XAFS using the exact spherical wave formula equation (15). Our results agree well with those of Rehr et al. (1986) for the case of Cu. The exact spherical wave double-scattering contribution to XAFS given by equation (20) does not separate into products of single-scattering contributions and is difficult to compute. Therefore, we use an approximate spherical wave approach when considering double and higher order multiple-scattering contributions to XAFS. Such a procedure greatly simplifies the numerical evaluation of multiple-scattering effects and provides a qualitative understanding of the important pathways that need to be considered. Our calculations of the multiple-scattering contributions for O_2 show convergence behavior that is similar to the exact SWMS calculations of Rehr et al. (1992). Therefore, we believe that approximate spherical waves for the higher order ($n > 1$) terms should be adequate for the purpose of analyzing astrophysical spectra.

Since one of our objectives was to produce simple models that get most of the physics correct, we have included a flag in the AXA tool that allows the user to reduce the number of parameters in a multiple-scattering expansion by using the single-scattering formula with amplitude and phase modification. We have computed the amplitude and phase modifications (Ω and ω) for oxygen due to the coherent sum of three multiple-scattering pathways. Significant amplitude enhancement occurs when the scattering angle is small. For these angles, it is extremely important to include multiple scattering into the model. Amplitude reduction also occurs as a result of multiple scattering. The capability for modeling multiple scattering using a small number of parameters should be a useful first step when analyzing astrophysical spectra.

5. CONCLUSION

We have presented a theoretical model and database designed to provide analysis of astrophysical XAFS. The theoretical model uses a hybrid treatment of exact spherical waves for single scattering and approximate spherical waves for multiple scattering. The model and database form the basis for the AXA tool, which we developed in order to analyze the properties of interstellar grains and molecules. The AXA tool extends our previous AEA tool (Woo et al. 1997) to include lower energies, and provides a foundation for further development of numerical XAFS models that may be needed to analyze the high-resolution X-ray spectra expected to be observed by future satellite missions (e.g., AXAF).

We would like to thank Alex Dalgarno for helpful comments and also the referee for calling our attention to several important articles. The work of R. C. F. was supported by the Division of Chemical Sciences, Office of Basic Energy Sciences, Office of Energy Research, US Department of Energy. The work of J. W. W. was supported by grant NAS 8-39073 from the National Aeronautics and Space Administration.

APPENDIX A

DERIVATION OF SWA

The angular momentum representation of the free propagator is given by (Lee & Pendry 1975; Ashley & Doniach 1975; Schaich 1973)

$$G_{lm,l'm'}(\boldsymbol{r}) = 4\pi \sum_{l''m''} \langle l\,m\,|\,l''m''\,|\,l'm'\rangle i^{l''} h_{l''}^{(+)}(kr) Y_{l''m''}(\hat{r}) , \quad (A1)$$

where $\langle l_1, m_1 | l_2, m_2 | l_3, m_3 \rangle$ is a Gaunt coefficient, which can be expressed in terms of Wigner 3-j symbols via

$$(-1)^{m_1}\langle l_1, -m_1 | l_2, m_2 | l_3, m_3 \rangle = \int Y_{l_1,m_1}(\theta, \phi) Y_{l_2,m_2}(\theta, \phi) Y_{l_3,m_3}(\theta, \phi) d\Omega$$
$$= \left[\frac{(2l_1+1)(2l_2+1)(2l_3+1)}{4\pi}\right]^{1/2} \begin{pmatrix} l_1 & l_2 & l_3 \\ 0 & 0 & 0 \end{pmatrix} \begin{pmatrix} l_1 & l_2 & l_3 \\ m_1 & m_2 & m_3 \end{pmatrix} . \tag{A2}$$

Using equations (A1) and (13) yields $g_{ll'}^{(|m|)}(x) = A_{ll'm}(x)/B_{ll'}$, where

$$A_{ll'}^{m}(x) = \sum_{l''} (2l''+1) \begin{pmatrix} l & l' & l'' \\ 0 & 0 & 0 \end{pmatrix} \begin{pmatrix} l & l' & l'' \\ -m & m & 0 \end{pmatrix} c_{l''}(x) , \tag{A3}$$

$$B_{ll'} = \sum_{l''} (2l''+1) \begin{pmatrix} l & l' & l'' \\ 0 & 0 & 0 \end{pmatrix} \begin{pmatrix} l & l' & l'' \\ 0 & 0 & 0 \end{pmatrix} . \tag{A4}$$

Equations (12) and (13) are used to obtain

$$\sum_{mm'} Z_{lm,l'm'}^{(1)} = 4\pi^2 \frac{\exp(2ikr)}{(kr)^2} Y_{l0}^*(-\hat{r}) Y_{l'0}(\hat{r}) \sum_{l''m''} (S_{l''} - 1) Y_{l''0}(-\hat{r}) Y_{l''0}^*(\hat{r}) g_{ll''}^{(m'')}(kr) g_{l''l'}^{(m'')}(kr) , \tag{A5}$$

which reduces to

$$\sum_{m} Z_{1m,1m}^{(1)} = 3 \frac{\exp(2ikr)}{(2ikr)^2} \sum_{l} (2l+1)(S_l - 1) P_l(\cos\pi)(|g_{l1}^{(0)}(kr)|^2 + 2|g_{l1}^{(1)}(kr)|^2) \tag{A6}$$

for the K-edge. The SWA result equation (14) is obtained by letting $l' = 1$ in equations (A3) and (A4) to get the radial functions needed by equation (A6)

$$g_{l1}^{(0)}(x) = \frac{(l+1)c_{l+1}(x) + l c_{l-1}(x)}{2l+1} , \tag{A7}$$

$$g_{l1}^{(1)}(x) = \sqrt{\frac{l(l+1)}{2}} \left[\frac{c_{l+1}(x) - c_{l-1}(x)}{2l+1}\right] . \tag{A8}$$

APPENDIX B

DERIVATION OF PWA

The PWA provides a conceptual basis for understanding the physical mechanisms that create XAFS. As an example, we provide a brief derivation of the double-scattering mechanism by assuming that the photoelectron wave function can be represented by plane waves in between each scattering center. The required plane waves are defined to be

$$\Psi(\boldsymbol{r}) = \Phi(\boldsymbol{r}_1) \exp(i\boldsymbol{k} \cdot \boldsymbol{R}_1) , \tag{B1}$$

$$\Psi'(\boldsymbol{r}) = \Phi'(\boldsymbol{r}_2) \exp(i\boldsymbol{k}' \cdot \boldsymbol{R}_2) , \tag{B2}$$

$$\Psi''(\boldsymbol{r}) = \Phi''(\boldsymbol{r} = 0) \exp(-i\boldsymbol{k}'' \cdot \boldsymbol{r}) , \tag{B3}$$

where $\boldsymbol{R}_j = \boldsymbol{r} - \boldsymbol{r}_j$, $\boldsymbol{r}_{12} = \boldsymbol{r}_2 - \boldsymbol{r}_1$, $\boldsymbol{k} = k\hat{r}_1$, $\boldsymbol{k}' = k\hat{r}_{12}$, and $\boldsymbol{k}'' = k\hat{r}_2$. The desired result is obtained by expanding the plane wave in equation (B3) and matching to

$$\Psi''(\boldsymbol{r}) = 2 \sum_{lm} Z_{lm,l'm'}^{(2)} j_l(kr) Y_{lm}(\hat{r}) , \tag{B4}$$

which yields

$$Z_{lm,l'm'}^{(2)} = 2\pi i^l Y_{lm}^*(-\hat{r}_2) \Phi''(\boldsymbol{r} = 0) . \tag{B5}$$

The plane wave amplitudes equations (B1)–(B3) are given by

$$\Phi(\boldsymbol{r}) = Y_{lm}(\hat{r}) h_l^{(+)}(kr) , \tag{B6}$$

$$\Phi'(\boldsymbol{r}) = \Phi(\boldsymbol{r}_1) \sum_{lm} 2\pi i^l (S_l - 1) Y_{lm}^*(\hat{r}_1) Y_{lm}(\hat{R}_1) h_l^{(+)}(kR_1) , \tag{B7}$$

$$\Phi''(\boldsymbol{r}) = \Phi'(\boldsymbol{r}_2) \sum_{lm} 2\pi i^l (S_l - 1) Y_{lm}^*(\hat{r}_{12}) Y_{lm}(\hat{R}_2) h_l^{(+)}(kR_2) . \tag{B8}$$

Equations (B6)–(B8) relate the amplitude of the interfering photoelectron to the amplitude of the original outgoing wave. Using the addition theorem for spherical harmonics yields

$$\Phi'(\boldsymbol{r}) = \Phi(\boldsymbol{r}_1)\tilde{f}(R_1, \theta_1)\frac{\exp(ikR_1)}{R_1}, \tag{B9}$$

$$\Phi''(\boldsymbol{r}) = \Phi'(\boldsymbol{r}_2)\tilde{f}(R_2, \theta_2)\frac{\exp(ikR_2)}{R_2}, \tag{B10}$$

where $\tilde{f}(r, \theta)$ is the effective spherical wave amplitude equation (19), θ_1 is the angle between $\boldsymbol{r}_1$ and $\boldsymbol{R}_1$, which arises from the first collision, and θ_2 is the angle between $\boldsymbol{r}_{12}$ and $\boldsymbol{R}_2$, which arises from the second collision. It is worth noting that although the derivation given above assumes plane wave behavior in between each collision, the amplitude equation (19) nevertheless retains some spherical wave character because of the function $c_l(kr)$. Using equations (B6), (B9), and (B10) yields

$$\Phi''(\boldsymbol{r} = 0) = Y_{lm}(\hat{r}_1)h_l^{(+)}(kr_1)\tilde{f}(r_2, \theta_2)\tilde{f}(r_{12}, \theta_1)\frac{\exp[ik(r_2 + r_{12})]}{r_2 r_{12}}, \tag{B11}$$

which reduces to

$$\Phi''(\boldsymbol{r} = 0) = (-i)^{l+1}Y_{lm}(\hat{r}_1)f(\theta_1)f(\theta_2)\frac{\exp[ik(r_1 + r_2 + r_{12})]}{kr_1 r_2 r_{12}} \tag{B12}$$

in the full PWA. Substituting equation (B11) and (B12) into equation (B5) yields the desired second-order result.

REFERENCES

Ashley, C. A., & Doniach, S. 1975, Phys. Rev. B, 11, 1279
Barton, J. J., & Shirley, D. A. 1985, Phys. Rev. B, 32, 1906
Evans, A. 1986, MNRAS, 223, 219
Filipponi, A., di Cicco, A., Tyson, T. A., & Natoli, C. R. 1991, Solid State Commun., 78, 265
Gurman, S. J., Binsted, N., & Ross, I. 1984, J. Phys. C, 17, 143
Hedin, L., & Lundqvist, S. 1969, Solid State Phys., 23, 1
Lee, P. A., & Beni, G. 1977, Phys. Rev. B, 15, 2862
Lee, P. A., & Pendry, J. B. 1975, Phys. Rev. B, 11, 2795
Martin, P. G. 1970, MNRAS, 149, 221
McKale, A. G., Veal, B. W., Paulikas, A. P., Chan, S.-K., & Knapp, G. S. 1988, J. Am. Chem. Soc., 110, 3763
Muller, J. E., & Schaich, W. L. 1983, Phys. Rev. B, 27, 6489
Mustre de Leon, J., Rehr, J. J., Zabinsky, S. I., & Albers, R. C. 1991, Phys. Rev. B, 44, 4146
Newville, M., Ravel, B., Haskel, D., Rehr, J. J., Stern, E. A., & Yacoby, Y. 1995, Physica B, 208–209, 154
Owens, A., Denby, M., Wells, A., Keay, A., Graessle, D. E., & Blake, R. L. 1997, ApJ, 476, 924
Rehr, J. J., & Albers, R. C. 1990, Phys. Rev. B, 41, 8139
Rehr, J. J., Albers, R. C., Natoli, C. R., & Stern, E. A. 1986, Phys. Rev. B, 34, 4350
Rehr, J. J., Albers, R. C., & Zabinsky, S. I. 1992, Phys. Rev. Lett., 69, 3397
Schaich, W. L. 1973, Phys. Rev. B, 8, 4028
Teo, B. K. 1985, EXAFS: Basic Principles and Data Analysis (Berlin: Springer)
Woo, J. W. 1995, ApJ, 447, L129
Woo, J. W., Forrey, R. C., & Cho, K. 1997, ApJ, 477, 235
Zabinsky, S. I., Rehr, J. J., Ankudinov, A., Albers, R. C., & Eller, M. J. 1995, Phys. Rev. B, 52, 2995